Applied Surface Science 301 (2014) 107–111

Contents lists available at ScienceDirect

Applied Surface Science

journal homepage: www.elsevier.com/locate/apsusc

Formation of multilayered scale during the oxidation of NiAl–Mo alloy

P.K. Ray*, M. Akinc, M.J. Kramer

Ames Laboratory and Department of Materials Science & Engineering Iowa State University, Ames IA 50011, USA

ARTICLE INFO

Article history:
Received 22 November 2013
Received in revised form 23 January 2014
Accepted 24 January 2014
Available online 31 January 2014

Keywords:
Mo–NiAl
High temperature alloys
Oxidation

ABSTRACT

We have studied the oxidation behavior of a hypereutectic NiAl–Mo alloy. This alloy showed an initial rapid mass loss followed by a relatively steady state behavior. The oxide scale formed during the oxidation process was seen to have a multilayered structure comprising of NiO, $NiAl_2O_4$, $NiMoO_4$ and Al_2O_3 with minor amounts of MoO_2 in the sub-scale region. The oxidation behavior is influenced significantly by the formation and stability of the constituent oxides, especially $NiMoO_4$. Hence the decomposition behavior of $NiMoO_4$ in the 1100–1200 °C was studied as well. The thermal decomposition of the $NiMoO_4$ was slow at 1100 °C, but accelerated at 1200 °C, resulting in the formation of NiO, which remained in the oxide scale, and MoO_3, which volatilized away.

1. Introduction

Nickel aluminides have been extensively studied as prospective high temperature oxidation resistant intermetallic compounds [1,2]. Pettit's work showed that β-NiAl to be an extremely oxidation resistant compound due to its high aluminum content [3]. He showed that the oxidation of this compound was characterized by the formation of a slow growing Al_2O_3 scale and the absence of NiO and $NiAl_2O_4$ over a long oxidation period. Kuznetsov investigated the ternary Ni–Al–O equilibrium at 1000 °C and explored the formation of various oxides and demonstrated that the $NiAl_2O_4$ spinel can exist in thermodynamic equilibrium with NiO, Al_2O_3 and Ni, but not with NiAl [4]. Trumble and Rühle studied spinel formation in diffusion bonded Ni/Al_2O_3 at 1390 °C [5]. From these studies, it was apparent that the β-NiAl could exist in thermodynamic equilibrium with only Al_2O_3 but not the spinel. On the other hand, the spinel exists in thermodynamic equilibrium with NiO, Al_2O_3 and the Ni rich solid solution.

The formation of $NiAl_2O_4$ spinel during high temperature oxidation in ambient atmosphere is an interesting phenomenon, given that previous studies have shown that spinel formation on bulk β-NiAl is a strong function of the oxygen partial pressure (p_{O_2}). So far, the reports indicate that $NiAl_2O_4$ can be formed on bulk β-NiAl only at very low values of p_{O_2} [6,7]. On the other hand, studies on oxidation of Ni–Al alloys having either relatively low Al content, or a ternary alloying addition, or both, have shown the formation of the spinel phase. For instance, Kuenzly and Douglass studied the oxidation of a Ni–Ni_3Al alloy with and without yttrium additions in the temperature range of 900–1200 °C. It was seen that NiO formed a part of the oxide scale. The $NiAl_2O_4$ spinel was also observed to form in the alloys containing 0.5 wt% yttrium [8]. Tjong studied the oxidation of a high activity β-NiAl coating on a γ phase Inconel 625 superalloy [9]. TEM studies following the oxidation at 1200 °C for as low as 250 s revealed the presence of a highly oriented NiO, $Ni(Al,Cr)_2O_4$ and α-$(Al,Cr)_2O_3$. The base Inconel alloy was presumably the source of chromium in the oxide scale. Strawbridge et al. studied the oxidation of dilute Ni base alloys and observed the formation of NiO in the scale as well [10]. Hindam and Smeltzer studied dilute Ni–Al alloys with low Al content (<6 wt% Al) and reported the formation of NiO and $NiAl_2O_4$ [11]. $NiAl_2O_4$ spinel can form by counter-diffusion of Ni and Al ions when Al_2O_3 and NiO are heated in contact with each other.

While oxidation of nickel aluminides generally result in an adhesive, slow growing protective Al_2O_3 scale, oxidation of molybdenum results in the formation of a volatile product, MoO_3, although MoO_2 can also form at low oxygen partial pressures [12,13]. Unlike nickel aluminides, where the steady state oxidation process is largely diffusion controlled, resulting in parabolic kinetics and low mass gain [1], oxidation of Mo is much more aggressive and follows linear kinetics, with significant mass loss [14]. Brenner studied the oxidation behavior of a binary Ni–Mo alloy and reported a formation of a triple layered structure, with NiO forming externally, $NiMoO_4$ forming in the middle layer and MoO_2 forming at the subscale region [15]. However, presence of high Al content has been known to suppress the formation of NiO in pure nickel aluminides resulting in an exclusive alumina scale [1,3]. Brenner's work suggested that alloys containing more than 20.6 at.% of Mo results in catastrophic oxidation. Our prior work on the isothermal kinetics

* Corresponding author. Tel.: +1 515 520 7356; fax: +1 515 294 5444.
E-mail addresses: prat@iastate.edu, pro.teak.ray@gmail.com (P.K. Ray).

0169-4332/$ – see front matter © 2014 Elsevier B.V. All rights reserved.
http://dx.doi.org/10.1016/j.apsusc.2014.01.148

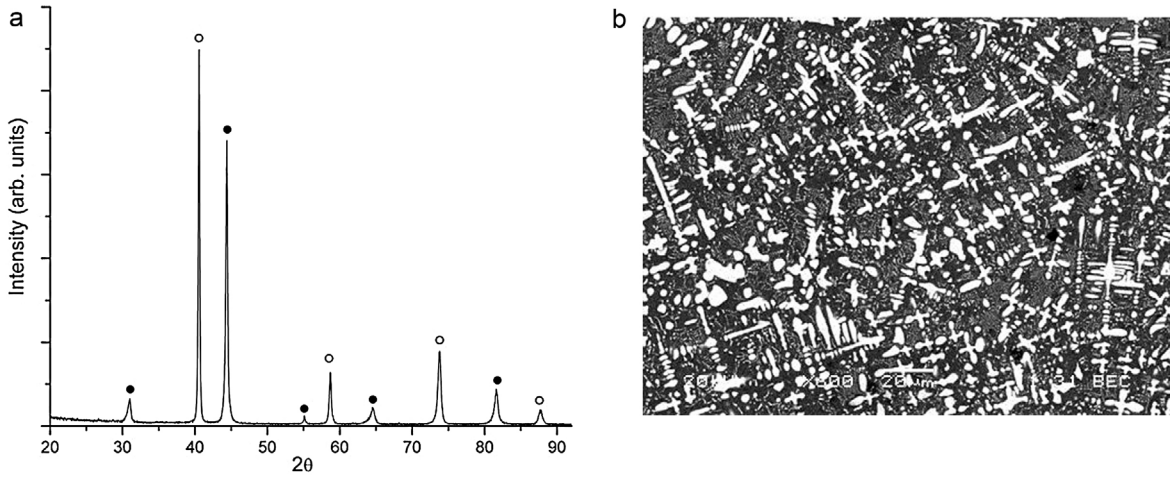

Fig. 1. (a) X-ray diffraction pattern of the NiAl–Mo alloy; (b) microstructure of the NiAl–Mo alloy.

of NiAl–Mo alloys showed that the mass loss rates in these alloys bear comparison with Mo–Si–B alloys at 1100 °C [15]. While the mass loss during the isothermal testing is relatively low, the oxide scale spallation when the oxidized coupons cool needs to be better understood, and this is the prime motivation for this study on the oxide scale development and oxidation behavior of such a NiAl–Mo alloy in the two phase (Mo + NiAl) region and thermal stability of the $NiMoO_4$ formed during this oxidation process.

2. Experimental

The alloys in the present study were prepared by arc melting of powder compacts. Pure elemental powders of Mo (Alfa Aesar, 99.5%), Ni (Materials Preparation Center, Ames Laboratory, 99.6%) and Al (Alfa Aesar, 99.8%) having a nominal composition $Ni_{40}Al_{40}Mo_{20}$ were mixed in appropriate ratios in a high energy SPEX 8000 mixer/shaker mill for 15 min and pelletized using a hydraulic press (Carver Inc.). The pellets were arc-melted in an ultra-high purity argon atmosphere (99.99% pure) on a water-cooled copper hearth using a Zr getter. The arc-melted buttons were then drop-cast into 10 mm diameter rods in a water-cooled cylindrical copper mold in an ultra-high purity argon atmosphere (99.95% pure). In order to better understand the oxidation behavior of this alloy, it was essential to know the thermal stability of the constituent phases in the oxide scale.

While the stabilities of most of the oxides observed are well studied, there is a relative paucity of data pertaining to the decomposition of $NiMoO_4$. Hence, we prepared $NiMoO_4$ by heating a pelletized mixture of Ni and Mo powders in equiatomic ratio at 900 °C for 24 h. X-ray diffraction of the oxidized product showed the formation of the α-$NiMoO_4$ compound. These powders were then heat treated for 2 h at different temperatures in ambient air, and the resulting products were studied using XRD to assess the phase changes that occurred in this process.

Alloy coupons for oxidation tests were cut from the drop-cast rods using a high speed saw equipped with an alumina blade. The isothermal oxidation tests were carried out at 1200 °C in ambient atmosphere for different time intervals. All the mass measurements were carried out *ex situ*. The coupons showed a tendency of significant spallation while cooling down to room temperature. The oxidized coupons were characterized using scanning electron microscopy. A JEOL 5910LV scanning electron microscope (SEM) was used to characterize the microstructures of the alloys. Semi-quantitative chemical analysis was done to identify the different phases in the microstructure using energy dispersive spectroscopy (EDS) (Noran-Vantage). Oxidized samples for scanning electron microscopy were prepared by first coating a thin layer of gold on the oxidized coupon. The coupon was then copper-plated electrolytically and cut to obtain cross-sections and polished for the SEM studies. X-ray diffraction (XRD) was carried out using an X-ray diffractometer (PANalytical, Philips) with a Bragg–Brentano geometry using a monochromatic Cu Kα radiation (wavelength = 1.54059 Å), with the data being collected over the range $2\theta = 20–80^\circ$.

3. Results

Fig. 1(a) shows the X-ray diffraction pattern of the NiAl–Mo alloy. It can be seen that the alloy consists of two phases–NiAl and Mo. The lattice parameters of NiAl and Mo were found to be 2.89 and 3.15 Å respectively. These values are very close to the reported values of the pure phases in these materials, indicating that there is fairly low dissolution of Mo in NiAl or Ni and Al in a Mo based solid solution. Fig. 1(b) shows the microstructure of the NiAl–Mo alloy. It can be seen that this alloy exhibits a two phase microstructure consisting primarily of Mo dendrites in a NiAl matrix with a significant amount of a lamellar NiAl–Mo eutectic in the inter-dendritic regions. This is in accordance with the reported NiAl–Mo pseudo binary phase diagram as well as our prior work on this system [16,17].

Fig. 2(a) shows the oxidation kinetics of this alloy at 1200 °C. It can be seen that there is a rapid initial mass loss, which gradually slows over time. The initial mass loss can be attributed to the formation of MoO_3 during the oxidation of the Mo phase. MoO_3 volatilizes above 700 °C [14] and deposits in the cooler sections of the furnace. As MoO_3 volatilizes, fresh surface of either Mo or NiAl is exposed to the oxidizing atmosphere, resulting in the formation of a number of other oxide phases. The presence of these oxide phases were detected using both XRD and SEM. As the oxidation coupons are taken out from the furnace, they rapidly cool and outer scale spalls off after cooling, while the inner layers of the oxide scale adhere to the surface. Fig. 2(b) shows the X-ray diffraction pattern from the spalled oxide scale while Fig. 2(c) shows the X-ray diffraction pattern of the oxidized surface. It can be seen that the spalled scale comprises primarily of NiO and $NiAl_2O_4$ and some amount of $NiMoO_4$. On the other hand, apart from the Mo and NiAl phases of the base alloy, $NiAl_2O_4$ and Al_2O_3 can be observed as the major phases in the diffraction pattern from the oxidized coupon surface.

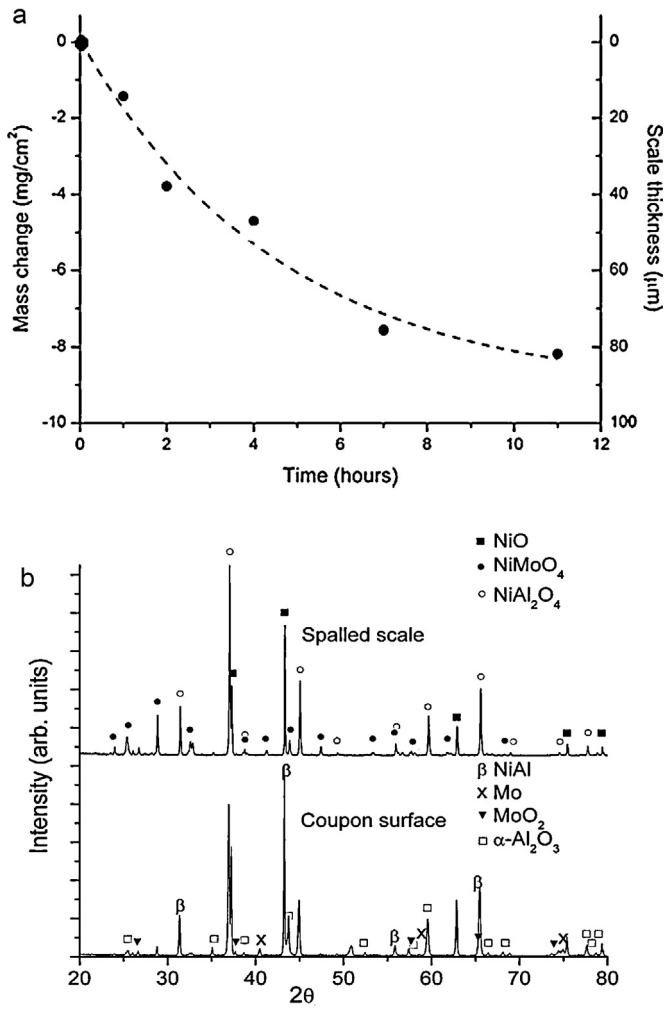

Fig. 2. (a) Isothermal oxidation kinetics at 1200 °C; (b) the upper X-ray diffraction pattern from the spalled scale; the lower X-ray diffraction pattern from the oxidized surface.

A microstructural investigation of the oxide scale cross-section was carried out in order to investigate the structure of the oxide scale, and the SEM results corroborate the evidence from the XRD studies. The oxidized microstructures are shown in Fig. 3(a). Fig. 3 shows a low magnification image of the oxide scale on the coupon surface. It can be seen that the oxide scale consists of multiple oxide layers. Fig. 3(b) shows a higher magnification image of a section of this scale, clearly highlighting the existence of multiple layers. EDS was employed to identify the individual layers. The upper layer indicates a Ni:Al ratio of 1:2 and is possibly the $NiAl_2O_4$ phase seen in the XRD pattern. This layer has minor bright regions entrapped that corresponds to a equiatomic Ni:Mo ratio, indicating the $NiMoO_4$ phase. The third layer exhibits a very dark contrast and was found to be alumina. In some sections, a subscale can be observed below the alumina layer, which consists of a mixture of primarily MoO_2 and a small amount of Al_2O_3.

The thermal stability of the $NiMoO_4$ phase was investigated using X-ray diffraction of heat-treated $NiMoO_4$ powders. Fig. 4(a) shows the diffraction pattern of the samples after heat treatment for 2 h in ambient atmosphere at different temperatures. Fig. 4(b) shows the variation in phase fraction of NiO and α-$NiMoO_4$ as a function of temperature after heat treatment in ambient air for two hours. It can be seen clearly that the relative phase fractions of NiO increases with an increase in temperature.

4. Discussion

The oxidation of this alloy starts with the individual phases, i.e. the Mo rich solid solution and the NiAl. In addition, there are two types of reactions occurring simultaneously: reaction between the oxides, and a reaction between the oxide and the base metal. It is postulated that the following reactions occur during the oxidation process:

$$Mo_{(s)} + 3/2O_{2(g)} \rightarrow MoO_{3(g)} \quad (1a)$$

$$2NiAl_{(s)} + 3/2O_{2(g)} \rightarrow Al_2O_{3(s)} + 2Ni_{(s)} \quad (1b)$$

$$MoO_{3(g)} + Ni_{(s)} + 1/2O_{2(g)} \rightarrow NiMoO_{4(s)} \quad (2a)$$

$$NiMoO_{4(s)} \rightarrow NiO_{(s)} + MoO_{3(g)} \quad (2b)$$

$$NiO_{(s)} + Al_2O_{3(s)} \rightarrow NiAl_2O_{4(s)} \quad (3)$$

$$Mo_{(s)} + O_{2(g)} \rightarrow MoO_{2(s)} \text{atlowpartialpressures} \quad (4)$$

Formation of MoO_3 during oxidation of Mo has been studied extensively [14,18,19], and it has been seen that MoO_3 volatilizes above 700 °C. A part of this MoO_3 formed at the surface volatilizes and deposits on the cooler section of the oxidation furnace, while the rest is available for reaction with other oxides or the base alloy in gaseous form. Oxidation of NiAl has been well studied as well [1,2], and this intermetallic is known to oxidize according to Reaction (1b). The $NiMoO_4$ formed during the oxidation process exists in two different structure types. The α-$NiMoO_4$ is the low temperature phase, while the β-$NiMoO_4$ is the high temperature phase. The

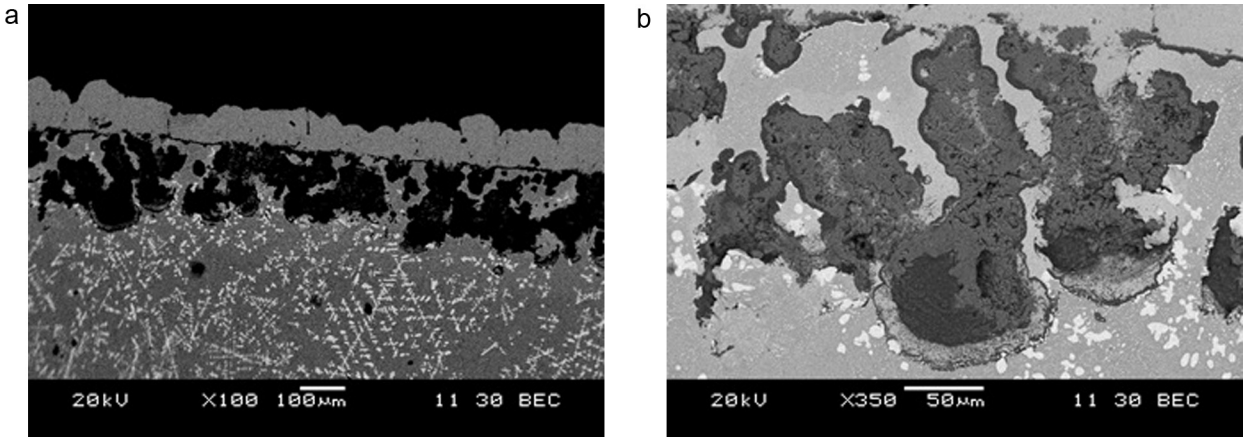

Fig. 3. (a) Low magnification image of the oxide scale; (b) higher magnification image of the oxide scale showing the multilayered structure.

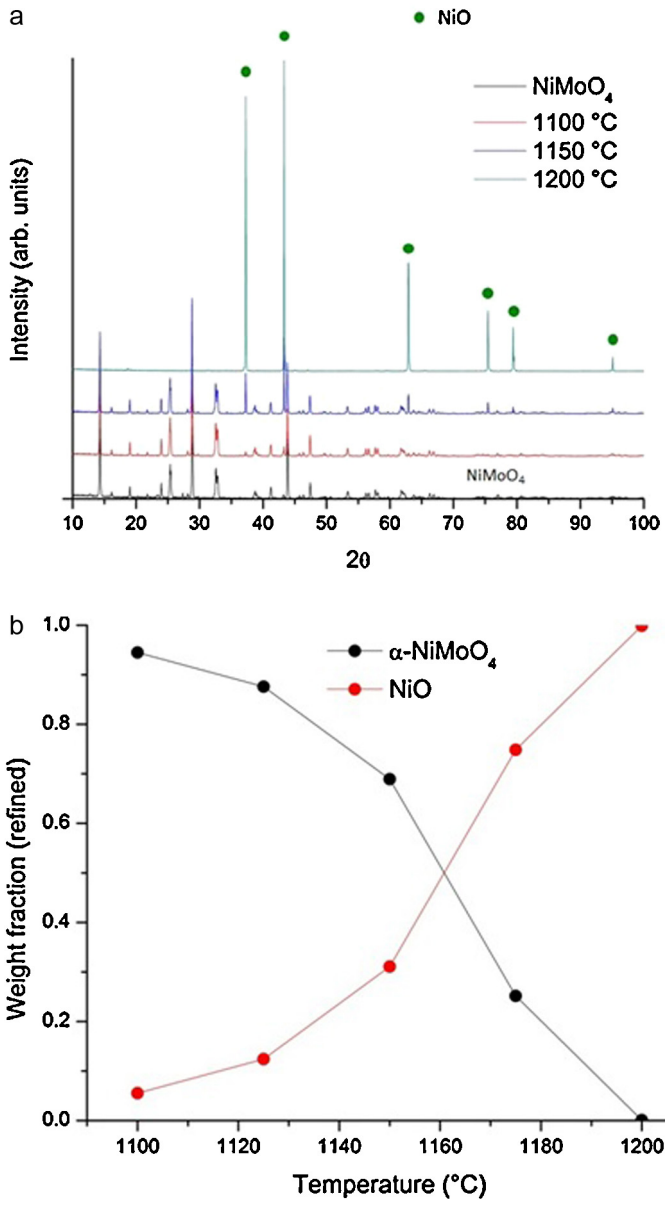

Fig. 4. (a) X-ray diffraction pattern of the $NiMoO_4$ samples after heat treatment for two hours at different temperatures; (b) phase fractions of NiO and $NiMoO_4$ as a function of temperature following 2 h of heat treatment.

$\alpha \rightarrow \beta$ transformation during the heating process occurs at approximately 700 °C and is known to be a reconstructive transformation that results in a change in the coordination of Mo ions [20]. The Mo ions are tetrahedrally coordinated in the β phase, as opposed to the octahedral coordination in α phase similar to β-(Fe, Co)MoO_4 [21]. The β-$NiMoO_4$ starts decomposing at 1100 °C. The rate of the decomposition reaction is a strong function of temperature. While the decomposition kinetics is quite sluggish at 1100 °C, they speed up rapidly as the temperature is increased to 1200 °C, (based on the phase fractions present after controlled heat treatments at different temperatures for two hours, as seen in Fig. 4(b)).

Oxidation of the NiAl phase has been studied extensively. NiAl oxidizes to form an exclusive alumina scale. Unlike nickel aluminides with low aluminum content like Ni_3Al, oxidation of NiAl does not result in the formation of NiO [1,2]. The abundance of aluminum and the high stability of alumina vis-à-vis NiO ensure that even if NiO forms, it gets reduced by the available aluminum. Therefore, the presence of NiO in the spalled scale could only be accounted for by the decomposition of $NiMoO_4$ at the outer layer, even if it forms. The $NiMoO_4$ formed deeper within the scale in small amounts, however, would be volumetrically constrained, preventing it from decomposing as easily as the $NiMoO_4$ in the outermost, unconstrained regions of the oxide scale. As the high temperature form β-$NiMoO_4$ cools, it transforms to the low temperature α-$NiMoO_4$ phase. While the phase transformation from $\alpha \rightarrow \beta$ occurs at 700 °C while heating, the reverse $\beta \rightarrow \alpha$ transformation occurs at approximately 250 °C. The volume change from $\alpha \rightarrow \beta$ during heating has been measured to be 5.5% [22]. While cooling, however, the large shrinkage of the α-$NiMoO_4$ unit cell parameters and a corresponding low shrinkage in the β-$NiMoO_4$ lattice parameters results in a much larger volume change, reported to be approximately 20% [22]. This huge volume change causes the oxide scale to spall off the coupon surface. This phenomenon accounts for the spallation of the oxide scale observed during the oxidation studies as the oxidized coupon was allowed to cool outside the furnace. This observation, in fact, is corroborated by Brenner on Ni–Mo alloys [15].

The $NiAl_2O_4$ spinel was observed at the top surface of the oxide scale adhering to the oxidized coupon. While the oxidation of NiAl does not yield $NiAl_2O_4$, it does result in the formation of a continuous alumina layer. When this alumina layer is in close proximity to the NiO formed in the outer layer formed by decomposition of $NiMoO_4$, they can sinter together, react and form the $NiAl_2O_4$ spinel at the interfacial region. This, therefore, explains the presence of the $NiAl_2O_4$ spinel as an interlayer between alumina and the topmost region of NiO. The alumina layer was identified as the α-Al_2O_3 from the X-ray diffraction patterns, which is to be expected, given the stability regime of α-Al_2O_3 is above 1100 °C [23]. In fact, the micrographs show the typical morphology associated with the α-Al_2O_3 phase [23]. The oxygen partial pressure below this alumina layer is likely to be extremely low. Therefore, if Mo rich features are present underneath the alumina layer, they can oxidize internally to form a partial MoO_2 subscale. Given the discontinuity of the Mo phase, this MoO_2 containing subscale could not form as a continuous layer, and was observed only in patches. Thus, a multilayered scale emerged during the oxidation process of the $Mo_{20}Ni_{40}Al_{40}$ alloy.

5. Conclusions

The present study showed that the oxidation of a two phase Mo–Ni–Al alloy resulted in the formation of a complex multilayered oxide scale comprising of a combination of the binary oxides NiO, Al_2O_3, MoO_2 and MoO_3 (which volatilizes) and the ternary oxides $NiAl_2O_4$ and $NiMoO_4$. The external layer in the scale comprises of $NiMoO_4$, as well as some NiO formed as a result of the decomposition of $NiMoO_4$ into the volatile MoO_3 and NiO. Beneath the external layer, $NiAl_2O_4$ layer is observed. $NiAl_2O_4$ has been known to form via a reaction between NiO and Al_2O_3. Given that the third layer comprises of α-Al_2O_3, it seems likely that the spinel formed primarily as an interphase layer between NiO and α-Al_2O_3. Normally, the formation and growth of NiO after prolonged oxidation is unexpected for high aluminum alloys. Nonetheless, the formation of NiO was observed in the present case, is due to the decomposition of $NiMoO_4$ at $T > 1100$ °C. As the coupon cools in contact with air, the $NiMoO_4$ can be expected to re-form in the temperature regime where it is stable. $NiMoO_4$ has been known to show massive volume change upon cooling (~20%). Therefore, during the cooling process, a significant fraction of the oxide scale containing $NiMoO_4$, NiO and some of the $NiAl_2O_4$ from the underlying layer spalled off. The oxidation behavior of this material is thus primarily governed by the formation and phase transformations of the $NiMoO_4$ in the oxide scale.

Acknowledgement

This work was supported by the DOE-FE (Crosscutting Research program) through Ames Laboratory contract no. DE-AC02-07CH11358.

References

[1] H.J. Grabke, Oxidation of NiAl and FeAl, Intermetallics 7 (10) (1999) 1153–1158.
[2] H.J. Grabke, M.W. Brumm, B. Wagemann, The oxidation of NiAl die oxidation von NiAl, Mater. Corros. 47 (12) (1996) 675–677.
[3] F.S. Petit, Oxidation mechanisms for Ni–Al alloys at temperatures between 900° and 1300 °C, Trans. Metall. Soc. AIME 239 (1967) 236.
[4] V. Kuznetsov, Aluminium–nickel–oxygen, in: Ternary Alloys, VCH, 1993, pp. 434–440.
[5] K.P. Trumble, M. Rühle, The role of oxygen for the spinel interphase formation at diffusion bonded Ni–Al_2O_3 interfaces, Z. Metallkd. 81 (1990) 749–755.
[6] E. Loginova, F. Cosandey, T.E. Madey, Nanoscopic nickel aluminate spinel ($NiAl_2O_4$) formation during NiAl(1 1 1) oxidation, Surf. Sci. 601 (3) (2007) L11–L14.
[7] E.D. Rodeghiero, J. Chisaki, E.P. Giannelis, In situ microstructural control of Ni/Al_2O_3 and Ni/$NiAl_2O_4$ composites from layered double hydroxides, Chem. Mater. 9 (2) (1997) 478–484.
[8] J.D. Kuenzly, D.L. Douglass, The oxidation mechanism of Ni_3Al containing yttrium, Oxid. Met. 8 (3) (1974) 139–178.
[9] S.C. Tjong, Transmission electron microscopy investigation of the transient oxides formed on the aluminide coating on Inconel 625 superalloy, Surf. Coat. Technol. 30 (2) (1987) 207–214.
[10] A. Strawbridge, F.H. Stott, G.C. Wood, The formation and incorporation into the scale of internal oxides developed during the high-temperature oxidation of dilute nickel-base alloys, Corros. Sci. 35 (5–8) (1993) 855–862.
[11] H.M. Hindam, W.W. Smeltzer, Growth and microstructure of α-Al_2O_3 on Ni–Al alloys: internal precipitation and transition to external scale, J. Electrochem. Soc. 127 (7) (1980) 1622–1630.
[12] D.O. Scanlon, et al., Theoretical and experimental study of the electronic structures of MoO_3 and MoO_2, J. Phys. Chem. C 114 (10) (2010) 4636–4645.
[13] T. Sekiya, Flux growth of MoO_2 single crystals, Mater. Res. Bull. 16 (7) (1981) 841–846.
[14] F.A. Rioult, et al., Transient oxidation of Mo–Si–B alloys: effect of the microstructure size scale, Acta Mater. 57 (15) (2009) 4600–4613.
[15] S.S. Brenner, Oxidation of iron–molybdenum and nickel–molybdenum alloys, J. Electrochem. Soc. 102 (1) (1955) 7–15.
[16] O. Kubaschewski, Aluminum–molybdenum–nickel, in: Ternary Alloys, VCH, 1993, pp. 199–218.
[17] P.K. Ray, et al., A multi-stage hierarchical approach to alloy design, JOM 62 (10) (2010) 25–29.
[18] V. Behrani, et al., Microstructure and oxidation behavior of Nb–Mo–Si–B alloys, Intermetallics 14 (1) (2006) 24–32.
[19] P. Mandal, et al., Oxidation behavior of Mo–Si–B alloys in wet air, Mater. Sci. Eng.: A 371 (1–2) (2004) 335–342.
[20] H. Ehrenberg, et al., Crystal and magnetic structure of α-$NiMoO_4$, J. Magn. Magn. Mater. 150 (3) (1995) 371–376.
[21] H. Ehrenberg, et al., A mixed transition metal molybdate, [beta]-($Co_{0.7}Fe_{0.3}$)MoO_4, Acta Crystallogr. C 55 (9) (1999) 1383–1384.
[22] E.Y. Tonkov, High Temperature Phase Transformations: A Handbook, Gordon and Breach, Rochester, 1992.
[23] I. Rommerskirchen, V. Kolarik, in: H.J. Grabke, M. Schutze (Eds.), Oxidation of Metals, Wiley-VCH, New York, 1998, pp. 109–120.